AFRL-RX-WP-JA-2014-0158

DENSITY FUNCTIONAL THEORY STUDY OF CHEMICAL SENSING ON SURFACES OF SINGLE-LAYER MOS_2 AND GRAPHENE (POSTPRINT)

Ruth Pachter
AFRL/RXA

APRIL 2014
Interim Report

AIR FORCE RESEARCH LABORATORY
MATERIALS AND MANUFACTURING DIRECTORATE
WRIGHT-PATTERSON AIR FORCE BASE, OH 45433-7750
AIR FORCE MATERIEL COMMAND
UNITED STATES AIR FORCE

NOTICE AND SIGNATURE PAGE

AFRL-RX-WP-JA-2014-0158 HAS BEEN REVIEWED AND IS APPROVED FOR PUBLICATION IN ACCORDANCE WITH ASSIGNED DISTRIBUTION STATEMENT.

//Signature//	//Signature//
RUTH PACHTER Senior Scientist Functional Materials Division	TIMOTHY J. BUNNING, Chief Functional Materials Division Materials and Manufacturing Directorate

REPORT DOCUMENTATION PAGE

Form Approved
OMB No. 074-0188

1. REPORT DATE (DD-MM-YYYY)	2. REPORT TYPE	3. DATES COVERED *(From – To)*
April 2014	Interim	28 March 2013 – 29 March 2014

4. TITLE AND SUBTITLE
DENSITY FUNCTIONAL THEORY STUDY OF CHEMICAL SENSING ON SURFACES OF SINGLE-LAYER MOS_2 AND GRAPHENE (POSTPRINT)

5a. CONTRACT NUMBER
FA8650-09-D-5430-0025

5b. GRANT NUMBER

5c. PROGRAM ELEMENT NUMBER
62102F

6. AUTHOR(S)
(see back)

5d. PROJECT NUMBER
4347

5e. TASK NUMBER

5f. WORK UNIT NUMBER
X0KU

7. PERFORMING ORGANIZATION NAME(S) AND ADDRESS(ES)
(see back)

8. PERFORMING ORGANIZATION REPORT NUMBER

9. SPONSORING / MONITORING AGENCY NAME(S) AND ADDRESS(ES)
Air Force Research Laboratory
Materials and Manufacturing Directorate
Wright Patterson Air Force Base, OH 45433-7750
Air Force Materiel Command
United States Air Force

10. SPONSOR/MONITOR'S ACRONYM(S)
AFRL/RXA

11. SPONSOR/MONITOR'S REPORT NUMBER(S)
AFRL-RX-WP-JA-2014-0158

12. DISTRIBUTION / AVAILABILITY STATEMENT
Distribution A. Approved for public release; distribution unlimited. This report contains color.

13. SUPPLEMENTARY NOTES
PA Case Number: 88ABW-2014-0840; Clearance Date: 3 March 2014. Journal article published in The Journal of Applied Physics 115, 164302 (2014). © 2014 AIP Publishing LLC. The U.S. Government is joint author of the work and has the right to use, modify, reproduce, release, perform, display or disclose the work. The final publication is available at http://dx.doi.org/10.1063/1.4871687.

14. ABSTRACT
In this work, density functional theory (DFT) calculations have been used to investigate chemical sensing on surfaces of single-layer MoS_2 and graphene, considering the adsorption of the chemical compounds triethylamine, acetone, tetrahydrofuran, methanol, 2,4,6-trinitrotoluene, o-nitrotoluene, o-dichlorobenzene, and 1,5-dicholoropentane. Physisorption of the adsorbates on free-standing surfaces was analyzed in detail for optimized material structures, considering various possible adsorption sites. Similar adsorption characteristics for the two surface types were demonstrated, where inclusion of a correction to the DFT functional for London dispersion was shown to be important to capture interactions at the interface of molecular adsorbate and surface. Charge transfer analyses for adsorbed free-standing surfaces generally demonstrated very small effects. However, charge transfer upon inclusion of the underlying SiO_2 substrate rationalized experimental observations for some of the adsorbates considered. A larger intrinsic response for the electron-donor triethylamine adsorbed on MoS_2 as compared to graphene was demonstrated, which may assist in devising chemical sensors for improved sensitivity.

15. SUBJECT TERMS
chemistry, computational, computer analysis, laser hardening, material development, nanotechnology, physics

16. SECURITY CLASSIFICATION OF:			17. LIMITATION OF ABSTRACT	18. NUMBER OF PAGES	19a. NAME OF RESPONSIBLE PERSON *(Monitor)*
a. REPORT	b. ABSTRACT	c. THIS PAGE			Ruth Pachter
Unclassified	Unclassified	Unclassified	SAR	12	19b. TELEPHONE NUBER *(include area code)* (937) 255-9689

REPORT DOCUMENTATION PAGE Cont'd

6. AUTHOR(S)

R. Pachter - Materials and Manufacturing Directorate, Air Force Research Laboratory, Functional Materials Division
F. Mehmood - General Dynamics Information Technology, Inc.

7. PERFORMING ORGANIZATION NAME(S) AND ADDRESS(ES)

AFRL/RXA
Air Force Research Laboratory
Materials and Manufacturing Directorate
Wright-Patterson Air Force Base, OH 45433-7750

General Dynamics Information Technology, Inc.
Dayton, Ohio 45431

JOURNAL OF APPLIED PHYSICS **115**, 164302 (2014)

Density functional theory study of chemical sensing on surfaces of single-layer MoS_2 and graphene

F. Mehmood and R. Pachter[a)]
Materials and Manufacturing Directorate, Air Force Research Laboratory, Wright-Patterson Air Force Base, Ohio 45433, USA

(Received 27 February 2014; accepted 29 March 2014; published online 22 April 2014)

In this work, density functional theory (DFT) calculations have been used to investigate chemical sensing on surfaces of single-layer MoS_2 and graphene, considering the adsorption of the chemical compounds triethylamine, acetone, tetrahydrofuran, methanol, 2,4,6-trinitrotoluene, o-nitrotoluene, o-dichlorobenzene, and 1,5-dicholoropentane. Physisorption of the adsorbates on free-standing surfaces was analyzed in detail for optimized material structures, considering various possible adsorption sites. Similar adsorption characteristics for the two surface types were demonstrated, where inclusion of a correction to the DFT functional for London dispersion was shown to be important to capture interactions at the interface of molecular adsorbate and surface. Charge transfer analyses for adsorbed free-standing surfaces generally demonstrated very small effects. However, charge transfer upon inclusion of the underlying SiO_2 substrate rationalized experimental observations for some of the adsorbates considered. A larger intrinsic response for the electron-donor triethylamine adsorbed on MoS_2 as compared to graphene was demonstrated, which may assist in devising chemical sensors for improved sensitivity. © *2014 AIP Publishing LLC*. [http://dx.doi.org/10.1063/1.4871687]

I. INTRODUCTION

Two-dimensional atomic crystals have recently emerged as an alternative to graphene, showing improved attributes in some cases.[1] Transition metal dichalcogenides have, in particular, drawn attention for application.[2] Recently, semiconducting single-layer MoS_2 (SL-MoS_2) field effect transistors (FETs) demonstrated some improvement in ON/OFF current ratio and relatively high mobilities,[3–6] however, transport could be complicated by localized states[7] or atmospheric adsorbates.[8] On the other hand, for practical applications, MoS_2 FETs emerged as promising for chemical sensing, e.g., of NO,[9,10] or NO_2 and NH_3.[11] Changes in conductance upon chemical adsorption on SL MoS_2 flakes in comparison to graphene for various analytes demonstrated a robust response.[12] A relatively large change in sensitivity was noted for the electron-donor triethylamine (TEA) by Perkins *et al.*,[12] while the response to electron-acceptors was minimal. SL-MoS_2 FETs are known to exhibit *n*-type doping although the origin of it remains mostly unclear, presumably due to impurities.[13] Unlike SL-MoS_2, SL-graphene is known to exhibit *p*-doping.[14,15] Indeed, as we previously pointed out,[16] understanding the behavior of a nano-FET is complicated by various scatterers, thus necessitating understanding of the intrinsic mechanism of an analyte's adsorption, which can achieved, in part, by computational prediction. Because MoS_2 could become a two-dimensional material of choice for chemical sensing, we aim in this work to systematically examine parameters that may affect the electronic structure upon molecular adsorption, both on MoS_2 and for comparison on graphene surfaces. Theoretical work has been limited so far, with a few examples for either adsorbates[14,17] or interaction with the substrate[15,18–20] for one type of surface, while MoS_2 vs. graphene has not been consistently assessed for chemical sensing application.

In this work, we applied density functional theory (DFT) for a comprehensive and consistent investigation of organic compound physisorption on model surface systems of graphene and MoS_2. Effects of inclusion of a SiO_2 substrate to model a realistic material were also examined for selected cases. Various adsorbates, including those used in the experimental work of Perkins *et al.*,[12] i.e., electron-donor and acceptor molecules, as well as solvents of varying polarity, were considered. Physisorption characteristics were analyzed in detail, where optimized hybrid material system structures were elucidated for the molecular adsorbates triethylamine, acetone (ACE), tetrahydrofuran, methanol, 2,4,6-trinitrotoluene (TNT), o-nitrotoluene, o-dichlorobenzene, and 1,5-dicholoropentane. Charge transfer analyses in the optimized surface—chemical adsorbate systems provided partial rationalization of observed sensing trends for some molecules upon inclusion of a substrate, and have shown that a MoS_2-based FET could potentially consist of a more sensitive platform for electron-donating chemical groups. Indeed, local density of states (LDOS) results demonstrated small effects upon adsorption, however, showing a relatively stronger response for an electron-donor upon inclusion of the underlying SiO_2 substrate.

II. COMPUTATIONAL DETAILS

DFT calculations[18,19] were carried out by solving the Kohn-Sham equations[19] using the Vienna ab initio simulation package (VASP).[20,21] The electron-ion interactions for Mo, S, C, O, N, Cl, and H were described by projector augmented plane wave (PAW) potentials.[22] A plane-wave energy cutoff of 400 eV was used for all calculations, found to be sufficient for these systems.[23] The generalized gradient

[a)]Author to whom correspondence should be addressed. Electronic address: ruth.pachter@us.af.mil

approximation (GGA) exchange-correlation functional of Perdew-Burke-Ernzerhof (PBE) was used,[24] and the vdW-DF[25] non-empirical correction was applied to correct for London dispersion upon molecular adsorption. Considering the large size of some of the molecules, a large 8×8 supercell was modeled with planar dimensions of 19.7×17.1 Å^2 for SL-graphene and 25.1×21.7 Å^2 for SL-MoS_2 surfaces. Brillouin zone sampling of the total energy was based on the technique by Monkhorst and Pack[26] with a k-point mesh of $3 \times 3 \times 1$, increased to $6 \times 6 \times 1$ for LDOS and charge transfer calculations. A k-point mesh of $5 \times 5 \times 1$ was used for structural optimization and total energy calculations for the MoS_2 and graphene surfaces on SiO_2 with a smaller cell, increased to $10 \times 10 \times 1$ for LDOS and charge calculations. A k-point mesh of $3 \times 3 \times 1$ for 2,4,6-trinitrotoluene on MoS_2 and graphene surfaces on SiO_2 was used because a larger cell was required. In calculation of the total energy of the system for a relaxed configuration, all atoms in a supercell were allowed to move in all directions and the structure was relaxed until the forces acting on each atom were converged to less than 0.01 eV/Å. Bader charge analyses[27] were used to analyze charge transfer.

III. RESULTS AND DISCUSSION

A. Physisorption on free-standing graphene and MoS_2 surfaces

First, we describe details of adsorption on graphene and MoS_2 surfaces. The graphene surface structure is shown in Fig. 1(a), having C-C bond lengths of 1.42 Å. MoS_2 has a closely packed layered structure with each Mo atom coordinated by six sulfur atoms in a trigonal prismatic unit, with Mo–S bond lengths of 2.40 Å (Fig. 1(b), side views Figs. 1(c) and 1(d)). Mo atoms in a plane between two planes are in 2-H stacking,[28] with S at a perpendicular distance of 3.16 Å. For each of the molecular adsorbates, namely, triethylamine, acetone, tetrahydrofuran methanol, 2,4,6-trinitrotoluene, o-nitrotoluene, o-dichlorobenzene, and 1,5-dicholoropentane, various adsorption sites were examined, as described below. The adsorption energy E_{ads} was derived by subtracting the total energy of any given molecule E_{mol} and that of the corresponding fully relaxed unadsorbed MoS_2 or graphene surface system E_{surf} from the total energy of the hybrid material system, namely, $(E_{mol/surf})$: $E_{ads} = E_{mol/surf} - E_{surf} - E_{mol}$.

Because the PBE functional does not account for London dispersion upon physisorption, the reported geometries and adsorption energies were calculated using the vdW-DF[25] non-empirical correction to the GGA functional, previously shown, for example, to be important for peptide aromatic residue adsorption.[16] Results using PBE with the vdW-DF correction indeed demonstrate a stronger relative adsorption, e.g., for 2,4,6-trinitrotoluene, as expected, as summarized in Table I. The optimized structures are depicted in Fig. 2. Distances of heavy atoms in the molecular moiety to the adsorbing surface are listed in Table II. Because the chemical structures are physisorbed on the surfaces we note that in all cases the internal structure of the molecule has been hardly perturbed.

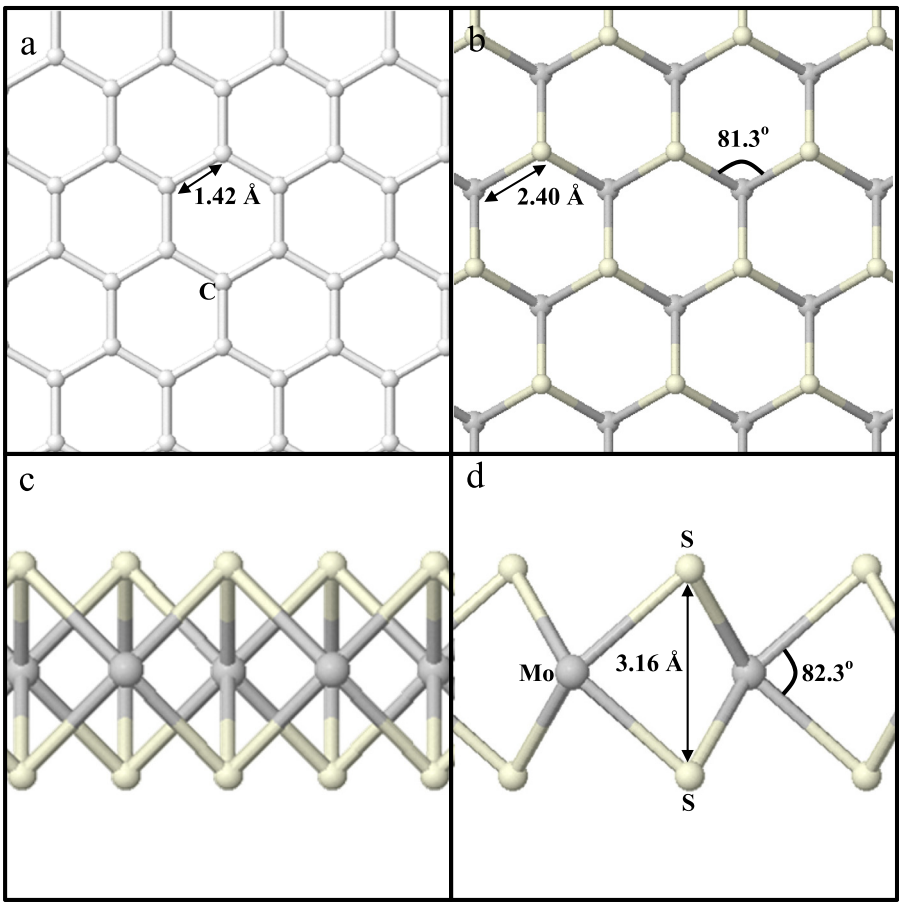

FIG. 1. The minimum energy structures of (a) graphene, (b)–(d) MoS_2 with two side views (c) and (d).

TABLE I. Adsorption energies (eV) of molecules on preferred adsorption sites (structures shown in Fig. 2), calculated with PBE and the vdW-DF non-empirical correction to the PBE functional.

	Graphene		MoS_2	
	PBE	PBE, vdW-corrected	PBE	PBE, vdW-corrected
Triethylamine	−0.05	−0.34	−0.08	−0.40
Acetone	−0.04	−0.26	−0.02	−0.26
Tetrahydrofuran	−0.05	−0.30	−0.03	−0.31
Methanol	−0.04	−0.14	−0.04	−0.16
2,4,6−trinitrotoluene	−0.10	−0.59	−0.05	−0.57
o−nitrotoluene	−0.06	−0.42	−0.04	−0.40
o-dichlorobenzene	−0.04	−0.37	−0.02	−0.37
1,5-dicholoropentane	−0.01	−0.46	−0.02	−0.48

Two sites for adsorption for triethylamine on graphene were analyzed, with the nitrogen atom in both starting configurations on top of graphene's carbon atom, but in one case the nitrogen and ethyl groups bent inwards and in the other outwards. The inward structure was slightly lower in energy, with a binding energy of −0.34 eV (Table I) as compared to −0.30 eV for outward adsorption. The molecule was displaced from its starting position, with the nitrogen atom moving from the (0, 0) top site to a position in the xy-plane (−0.34, 0.23 Å) (see structure in Fig. 2(a)). On MoS_2, the site with the nitrogen atom and ethyl groups of triethylamine pointing outwards was preferred by 0.03 eV. The molecule undergoes significant motion and was transferred from an initial position on top of a sulfur atom to a hollow site (Fig. 2(b)). Optimized distances of the nitrogen atom to the surfaces are somewhat shorter for graphene as compared to MoS_2 (4.44 Å vs. 4.63 Å, respectively, in Table II). Stronger adsorption is noted on the MoS_2 surface, of −0.40 eV.

In adsorption of acetone, investigated for five nonequivalent sites, a different behavior for the two surfaces is shown. Adsorption sites considered included the oxygen atom positioned on the top, bridge and hollow sites and central CO parallel to the surface, and in another case the oxygen atom pointed away from the surface. The preferable adsorption site on the graphene surface (so-called CO-flat, shown in Fig. 2(a)) resulted in a binding energy of −0.26 eV (Table I), while a top site with adsorption energy of −0.19 eV was the next strongest adsorbed structure. In this case, the CO bond is no longer parallel to the surface, but the O atom is slightly tilted toward the graphene C atom at a distance of 5.96 Å (Table II). Similarly, the CO bonds of acetone on the top, bridge and hollow sites do not stay perpendicular to the graphene surface upon relaxation but are tilted with a slightly smaller angle than the most preferred site (CO-flat). On MoS_2, the on-top site is slightly preferred by 0.03 eV, as compared to the CO-flat site. Examination of the structures indicated small differences between the two sites, with an O–S bond distance ($d_{O\text{-}S}$) of 0.14 Å, which is smaller than for the most preferred adsorption site. Fig. 2(b) shows the minimum energy structure, and the corresponding distance (Table II) demonstrates closer proximity to the surface than for graphene. The adsorption energies for the remaining three sites were in the range of −0.13–−0.16 eV.

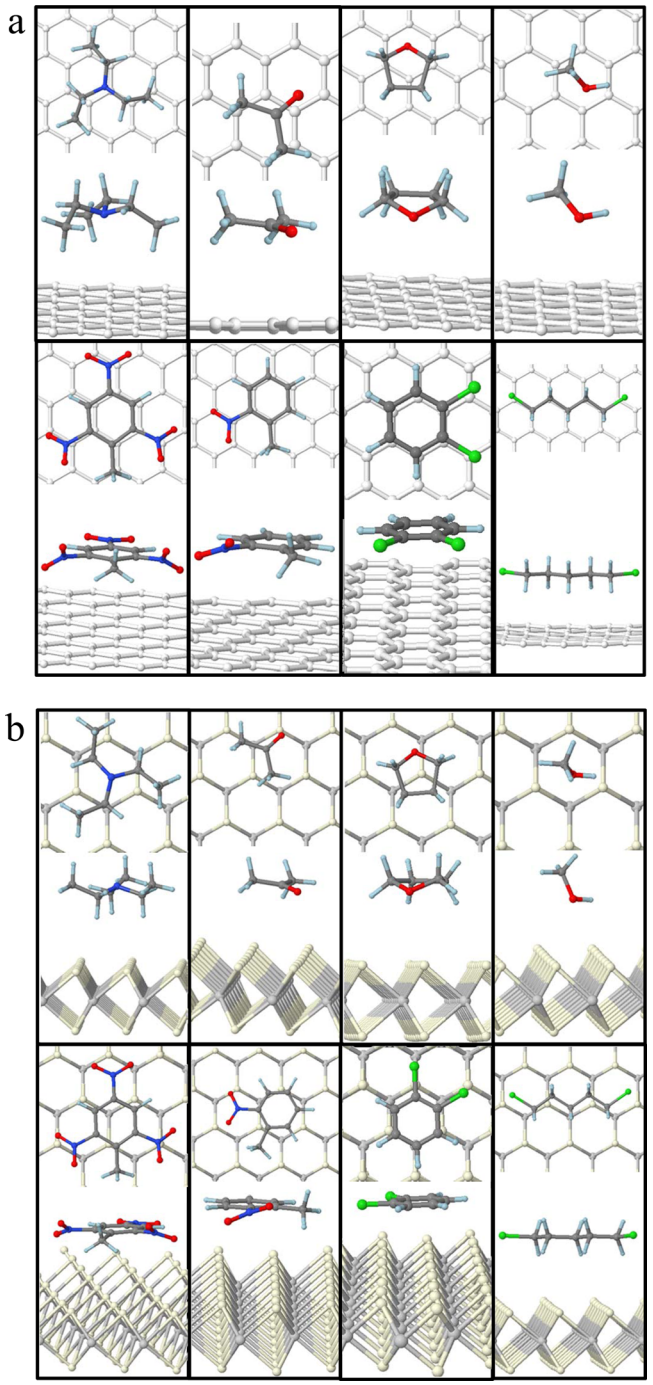

FIG. 2. Top and side views of adsorbed triethylamine, acetone, tetrahydrofuran, methanol (left to right top panel) and 2,4,6-trinitrotoluene, o-nitrotoluene, o-dichlorobenzene and 1,5-dicholoropentane (bottom panel left to right, respectively) on (a) graphene and (b) MoS_2 surfaces.

For tetrahydrofuran, with out-of-plane oxygen atom in the ring structure, we considered four distinct sites for adsorption. Two sites consider adsorption in a perpendicular direction through the oxygen atom on top and hollow sites on the surface, while the remaining two sites consider planar adsorption parallel to the surface with the center of the tetrahydrofuran ring aligned with the graphene ring (planar-top site) and the center of the tetrahydrofuran on top of the C

TABLE II. Distances (Å) of adsorbed molecules for preferred adsorption sites on graphene and MoS_2 surfaces.

	Triethylamine	Acetone	Tetrahydrofuran	Methanol	2,4,6-trinitrotoluene	o-nitrotoluene	o-dichlorobenzene	1,5-dicholoropentane
Graphene								
d_{G-C1}	4.89	3.78	4.05	4.21	4.04	4.09	4.02	3.40
d_{G-C2}	…	4.78	…	…	…	…	…	…
d_{G-C3}	…	4.30	…	…	…	…	…	…
d_{G-O}	…	5.96	3.41	3.37	…	…	…	…
d_{C-C}	1.53	1.51	1.54	…	1.41	1.41	1.40	1.52
d_{C-O}	…	1.23	1.43	1.43	…	…	…	…
d_{C-H}	1.10	1.10	1.11	1.11	1.09	1.09	1.09	1.11
d_{C-Cl}	…	…	…	…	…	…	1.73	1.80
d_{G-Cl}	…	…	…	…	…	…	…	3.40
d_{C-N}	1.47	…	…	…	1.47	1.47	…	…
d_{N-O}	…	…	…	…	1.24	1.24	…	…
d_{G-N}	4.44	…	…	…	4.04	…	…	…
d_{O-H}	…	…	…	0.97	…	…	…	…
MoS_2								
d_{S-C1}	4.17	4.08	3.92	4.55	3.75	4.06	3.94	4.00
d_{S-C2}	4.52	4.01	…	…	…	…	…	…
d_{S-C3}	…	4.08	…	…	…	…	…	…
d_{S-O}	…	3.53	3.54	3.31	…	…	…	…
d_{C-C}	1.53	1.51	1.55	…	1.42	1.40	1.40	1.52
d_{C-O}	…	1.23	1.43	1.43	…	…	…	…
d_{C-H}	1.11	1.10	1.11	1.11	1.09	1.09	1.09	1.11
d_{C-Cl}	…	…	…	…	…	…	1.74	1.80
d_{S-Cl}	…	…	…	…	…	…	…	4.09
d_{C-N}	1.47	…	…	…	1.48	1.48	…	…
d_{N-O}	…	…	…	…	1.24	1.24	…	…
d_{S-N}	4.63	…	…	…	3.78	…	…	…
d_{O-H}	…	…	…	0.97	…	…	…	…

atom of graphene (planar-hollow site). Planar adsorption sites were of lower energy, and among those the planar-hollow site was slightly preferred. The adsorption energy of tetrahydrofuran on graphene was −0.30 eV (Table I) and the structure is shown in Fig. 2(a). For MoS_2, a similar structure was found to be a minimum energy structure (Fig. 2(b)) with an adsorption energy of −0.31 eV (Table I). Distances to the surfaces are generally comparable (Table II), although somewhat shorter to the MoS_2 surface.

Six adsorption sites for methanol on graphene and MoS_2 were investigated, through either the oxygen or carbon atom on top, bridge and hollow sites. In Fig. 2(a), we show the adsorption of methanol at the oxygen atom on a graphene hollow site, although adsorption on all studied sites was similar, with binding energies of ca. −0.12−−0.14 eV. However, for the MoS_2 surface, preference for methanol adsorption on a hollow site through an oxygen atom was calculated (Figure 2(b)), with a binding energy of −0.16 eV. Earlier calculations using a vdW-DF correction to PBE showed comparable magnitudes and site preferences for adsorption.[17]

Adsorption of 2,4,6-trinitrotoluene and o-nitrotoluene was modeled such that the benzene rings were placed on top of a graphene ring. During relaxation, the 2,4,6-trinitrotoluene molecule moved slightly inward as compared to o-nitrotoluene, and a fully relaxed molecule was at a distance of 4.04 Å and 3.78 Å from the graphene and MoS_2 surfaces, respectively (Table II and Fig. 2). o-nitrotoluene dislocated slightly in the xy-plane and moved outward in the z-direction during relaxation. The optimized structure was at a distance of 4.09 Å from the graphene surface, with a similar value for MoS_2 (Table II). Unlike for graphene, the C-NO_2 and C-CH_3 bonds did not stay aligned to the Mo-S bonds of MoS_2 (Fig. 2(b)). Larger adsorption energies were calculated for stacked configurations on the surfaces (Table I).

o-dichlorobenzene adsorption was similarly modeled on graphene and MoS_2, initially placed at 3.00 Å away from the graphene surface. It moved farther from the surface (4.02–4.05 Å) upon relaxation, with a binding energy of −0.37 eV. For adsorption on single-wall carbon nanotubes, top ring adsorption was predicted to be the most preferred site with binding energies of the same order.[29] Similar to graphene, o-dichlorobenzene prefers a top ring site on the MoS_2 surface. The MoS_2 Mo-S ring is larger than benzene, and therefore, o-dichlorobenzene lies within larger Mo-S ring with a binding energy similar to that for graphene (Table II and Fig. 2).

Three sites for 1,5-dicholoropentane adsorption were studied on graphene, specifically adsorbed parallel to the graphene surface with two, three and five out of the five carbon atoms pointing inward. We found that the site that has all five carbon atoms of 1,5-dicholoropentane aligned parallel to the graphene surface showing the strongest binding energy, of −0.46 eV, next to the site with three carbon atoms bound

TABLE III. Accumulation (+) and depletion (−) of charge (e) for molecular adsorbates on free-standing graphene and MoS_2 surfaces.

	Graphene	MoS_2
Triethylamine	−0.003 (−0.128)[a]	−0.001 (−0.250)[a]
Acetone	0.005 (0.037)[a]	−0.039 (−0.147)[a]
Tetrahydrofuran	0.002	−0.021
Methanol	−0.001	0.002
2,4,6−trinitrotoluene	0.140 (0.017)[a]	0.038 (0.031)[a]
o-nitrotoluene	0.006	0.009
o-dichlorobenzene	−0.001	0.037
1,5-dicholoropentane	0.005	0.012

[a]Results for SiO_2-supported graphene and MoS_2 surfaces.

to the surface (−0.43 eV). This implies a stronger binding energy with a larger number of alignment of the bonds. We found this to hold for the MoS_2 surface too. A slightly stronger bound 1,5-dicholoropentane (by ∼0.02 eV) stayed relatively far from the MoS_2 surface with a S–C bond length ($d_{S\text{-}C}$) of 4.00 Å, as compared to a graphene–C distance ($d_{G\text{-}C}$) of 3.40 Å (Table II).

B. Charge transfer upon chemical adsorption

Comparing changes in charge transfer upon molecular adsorption to the relative conductivity change of a nano-FET is complicated because of consideration of only one molecule in the calculations, and lack of consideration of impurities or defects.[16,23] However, in this work, we seek an intrinsic response of the surface to molecular adsorption. Bader charge analyses are summarized in Table III. Charge transfer on free-standing surfaces demonstrate small changes, of 0.00–0.04 e except for 2,4,6-trinitrotoluene, consistent with physisorbed adsorbates in other work.[14] Note that, for example, for triethylamine and acetone, these small values are consistent with the corresponding distances of the nitrogen and oxygen atoms to the surfaces, respectively (Table II). Triethylamine and acetone had no noticeable effect on shifting the Dirac point away from the Fermi level in the LDOS for the graphene surface because of the minimal charge transfer (Fig. 3). Results for the MoS_2 surface for triethylamine and acetone similarly show a small response (Figs. 4(a) and 4(b)). On the other hand, charge transfer to 2,4,6-trinitrotoluene was calculated to be somewhat larger than for other adsorbates (Table III), as expected. The removal of charge from the graphene surface upon adsorption of the strong electron-acceptor will consequently shift the Dirac point in LDOS away from the Fermi level towards higher energies (conduction band), as shown in Fig. 3, while the LDOS of MoS_2 in Fig. 4 also show a small shift around the Fermi level.

Experimentally, however, robust sensitivity was indicated for triethylamine, a laboratory-safe decomposition product from the V-series of nerve gas agents, and also acetone, particularly for MoS_2.[12] To explore potential interactions with the underlying SiO_2 substrate that may explain this behavior, charge transfer for surfaces on silica was considered for selected cases. A model based on α-quartz was considered, because it represents the local character of SiO_2's amorphous structure,[30] as previously rationalized.[31] It

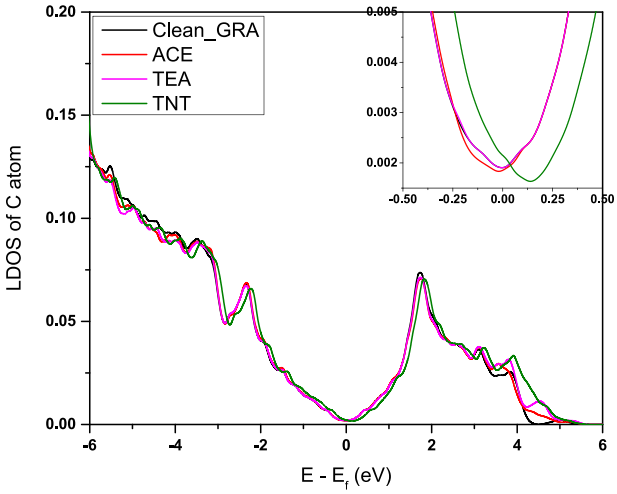

FIG. 3. LDOS of carbon atom for free-standing graphene (black line) compared with carbon atom of graphene with adsorbed TEA, ACE, and TNT. Inset shows the enlarged version of Dirac point shift for supported graphene.

was shown that differences in adsorption of graphene on a SiO_2 substrate based on α-quartz or cristobalite models are small,[30] and because our goal was to understand relative changes upon molecular adsorption, only one type of surface was evaluated. It was pointed out[31] that experimental and theoretical studies showed that the upper subsurfaces of cleaved SiO_2 undergo surface reconstruction that results in

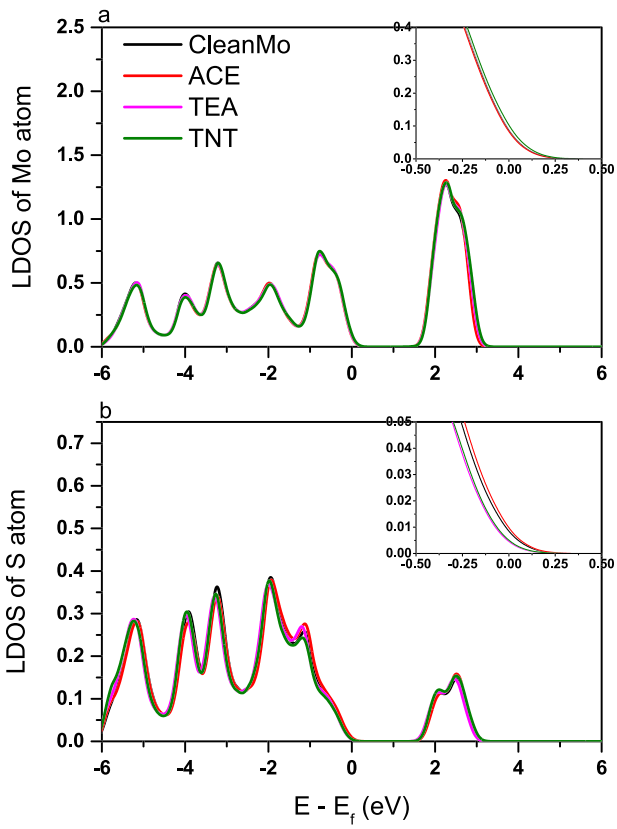

FIG. 4. LDOS of (a) Mo atom and (b) S atom of free-standing MoS_2 surface (black line) compared with Mo atom of MoS_2-surface with an adsorbed TNT molecule. Insets show the enlarged version of the plot around Fermi energy showing a shift in the LDOS.

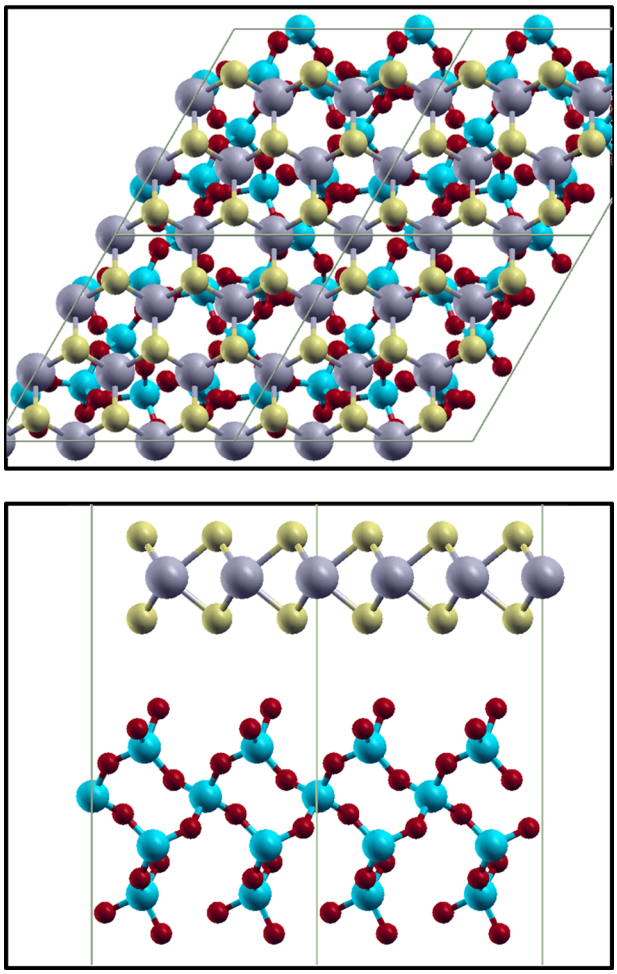

FIG. 5. A top (a) and side view (b) of MoS_2 on SiO_2 substrate.

oxygen-terminated surfaces.[32] It was also shown that the optimized structures of graphene on oxygen-terminated or hydroxylated (0001) SiO_2 surfaces are similar.[31] We note that comparing to an experimental *n*-type device,[12] presumably due to defects and impurities as shown in recent theoretical work,[15] it is unlikely that there are silanol groups on the SiO_2 surface. We therefore considered an oxygen-terminated α-quartz SiO_2 surface.

The choice to model the substrate by a (0001) α-quartz surface was additionally based on the small lattice mismatch for both MoS_2 and graphene surfaces. The optimized structure of the α-quartz SiO_2 model structure resulted in Si-O bond lengths between 1.62–1.65 Å with a Si-O-Si bond angle of 142.6°, in agreement with earlier calculations.[30] The calculated lattice constant for graphene was 2.46 Å, and therefore, a 4×4 cell of graphene (32 C atoms) was adsorbed on a 2×2 cell of (0001) SiO_2, leading to a lattice mismatch of ∼3%. A 2×2 cell with four layers of α-quartz SiO_2 terminated with oxygen was modeled with a vacuum region of 20 Å. The lattice parameter of α-quartz SiO_2 was calculated as 4.85 Å and for MoS_2 was 3.20 Å. A 3×3 cell of MoS_2 (9 Mo and 18 S atoms) was therefore adsorbed on a 2×2 cell of (0001) SiO_2 (16 Si and 40 O atoms), leading to a lattice mismatch of ∼2%. The small strain was shown not to affect the electronic properties.[15] For computational feasibility, the cell size was reduced by almost a half from what we used for the unsupported graphene and MoS_2 surfaces. Optimized distances between the top layer of SiO_2 and the adsorbed surfaces were 2.85 Å for graphene and 2.97 Å for MoS_2 (shown in Fig. 5 for MoS_2). Charge densities for graphene and MoS_2 on SiO_2 are shown in Figs. 6(a) and 6(b), respectively.

The SiO_2 substrate causes *p*-doping by 1.071 e and 0.738 e of graphene and MoS_2 surfaces, respectively. As a consequence of the graphene *p*-doping, which is consistent with results for cristobalite SiO_2,[14] the Dirac point of the LDOS is shifted from valence band towards the higher energies (conduction band) by 1.15 eV, as shown in Fig. 7. The LDOS of Mo and S atoms for the MoS_2 surface on SiO_2 are shown in Figs. 8(a) and 8(b), demonstrating a shift of the band gap of

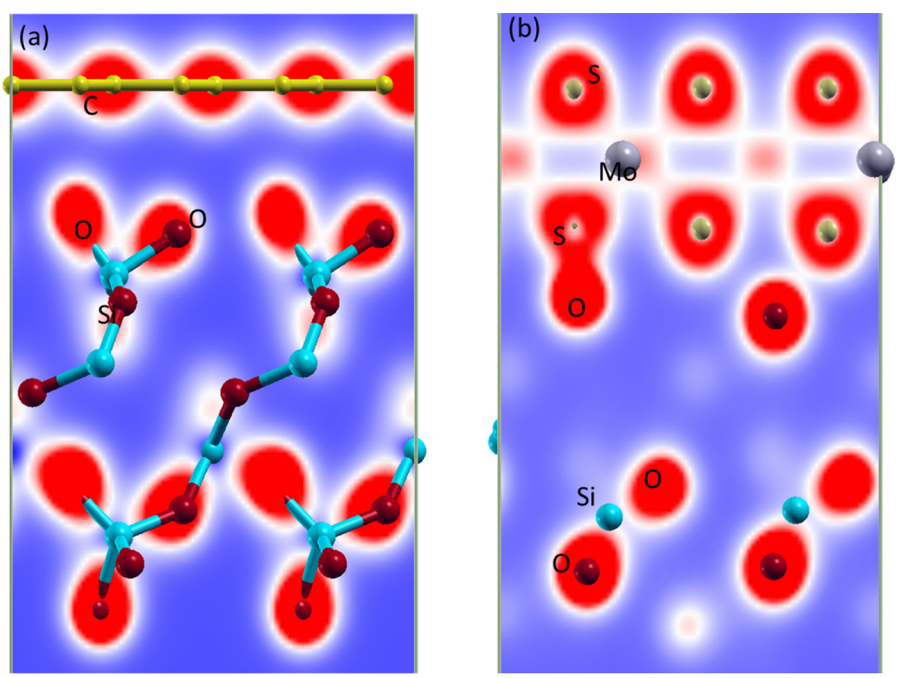

FIG. 6. Surface contour plots of charge densities for graphene and MoS_2 adsorbed on SiO_2 plotted along a plane passing through the center of (a) carbon of graphene, silicon, and oxygen atoms and (b) molybdenum, sulfur, silicon, and oxygen atoms.

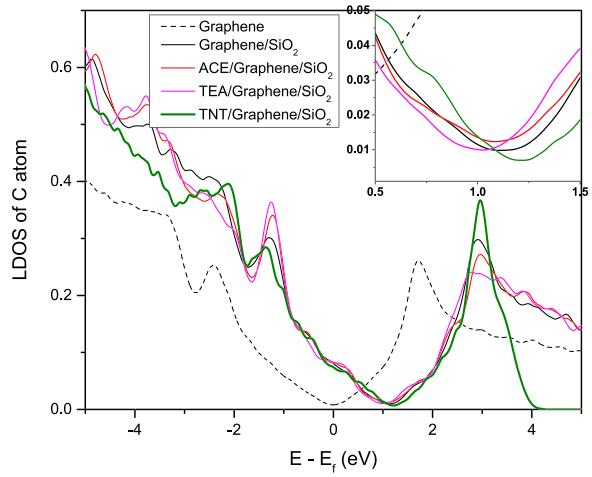

FIG. 7. LDOS of carbon atom of free-standing graphene (dashed black line) and supported graphene (solid black line) with TEA and ACE. Inset shows the enlarged version of Dirac point shift.

about 0.25 eV, consistent with the charge transfer. This response affects, in turn, changes in charge transfer upon molecular adsorption, for example, the electron-accepting 2,4,6-trinitrotoluene molecule shows accumulation of charge on free-standing surfaces of graphene and MoS_2. Charge transfer, however, to graphene and MoS_2 surface with the SiO_2 substrate is smaller, because of the *p*-doping of the surfaces, as expected.

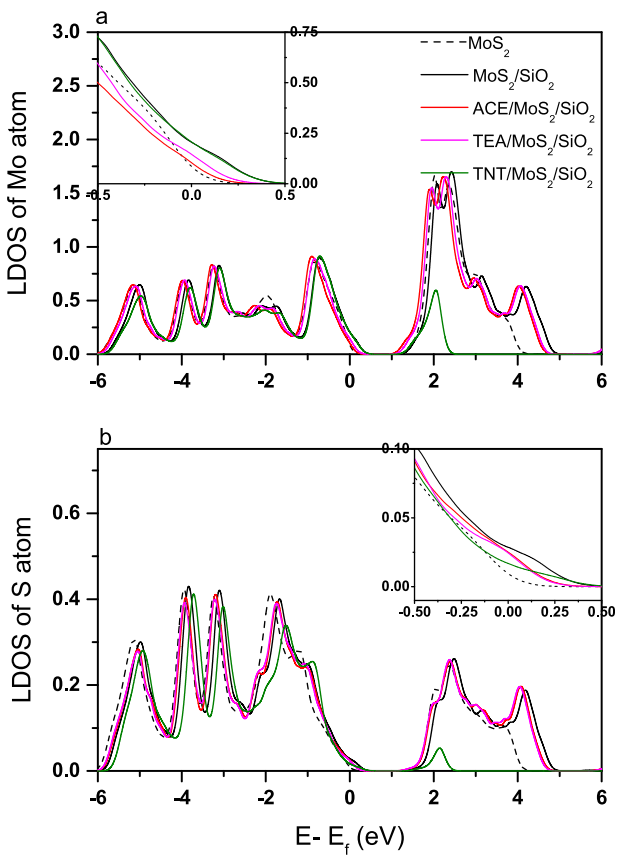

FIG. 8. LDOS of Mo atom (a) and sulfur atom (b) for free-standing MoS_2 (dashed line) and supported MoS_2 with adsorbed TEA and ACE. Inset shows the enlarged version of LDOS around Fermi-level.

On the other hand, depletion of charge on triethylamine for adsorption on both graphene and MoS_2 surfaces modeled on a substrate is noted, of 0.128 e and 0.250 e, respectively (see Table III), as well as for acetone on MoS_2 (e.g., 0.147 e on MoS_2, Table III, however, inconclusive for graphene). Interestingly, the intrinsic effect is stronger for MoS_2, qualitatively consistent with experimental observations.[12] A smaller Dirac point shift because of a smaller charge transfer for the system with the triethylamine and acetone on graphene is noted in Fig. 7. Because triethylamine and acetone *n*-dope the SiO_2-supported MoS_2 surface more significantly, the LDOS shift towards the valence band (lower energies) upon triethylamine adsorption (Fig. 8) is more noticeable compared to graphene.

IV. CONCLUSIONS

In this work, we investigated by DFT calculations the physisorption of the molecular adsorbates triethylamine, acetone, tetrahydrofuran, methanol, 2,4,6-trinitrotoluene, o-nitrotoluene, o-dichlorobenzene, and 1,5-dicholoropentane on surfaces of single-layer MoS_2 and graphene, in order to understand parameters that may affect the intrinsic response for chemical sensing application. Detailed investigation of adsorption sites for the hybrid material systems, and correction for London dispersion in the DFT functional, assured accuracy of the calculated adsorption energies. Charge transfer analyses and LDOS results for the optimized surface with chemical adsorbates demonstrated very small effects. However, inclusion of an underlying SiO_2 substrate model surfaces in some cases, provided rationalization of the observed sensing for triethylamine, for example. These results may assist in devising chemical sensors for improved sensitivity.

ACKNOWLEDGMENTS

Support for this work was provided by the Air Force Office of Scientific Research through a National Research Council (NRC) postdoctoral fellowship. The AFRL DoD Supercomputing Resource Center is acknowledged for providing computational resources and helpful support.

[1]S. Z. Butler *et al.*, ACS Nano **7**, 2898 (2013).
[2]Q. H. Wang, K. Kalantar-Zadeh, A. Kis, J. N. Coleman, and M. S. Strano, Nat. Nanotechnol. **7**, 699 (2012).
[3]D. Jariwala, V. K. Sangwan, D. J. Late, J. E. Johns, V. P. Dravid, T. J. Marks, L. J. Lauhon, and M. C. Hersam, Appl. Phys. Lett. **102**, 173107 (2013).
[4]N. R. Pradhan, D. Rhodes, Q. Zhang, S. Talapatra, M. Terrones, P. M. Ajayan, and L. Balicas, Appl. Phys. Lett. **102**, 123105 (2013).
[5]S. Das, H.-Y. Chen, A. V. Penumatcha, and J. Appenzeller, Nano Lett. **13**, 100 (2013).
[6]B. Radisavljevic, A. Radenovic, J. Brivio, V. Giacometti, and A. Kis, Nat. Nanotechnol. **6**, 147 (2011).
[7]S. Ghatak, A. N. Pal, and A. Ghosh, ACS Nano **5**, 7707 (2011).
[8]V. K. Sangwan, H. N. Arnold, D. Jariwala, T. J. Marks, L. J. Lauhon, and M. C. Hersam, Nano Lett. **13**, 4351 (2013).
[9]H. Li *et al.*, Small **8**, 63 (2012).
[10]Q. He, Z. Zeng, Z. Yin, H. Li, S. Wu, X. Huang, and H. Zhang, Small **8**, 2994 (2012).
[11]D. J. Late *et al.*, ACS Nano **7**, 4879 (2013).
[12]F. K. Perkins, A. L. Friedman, E. Cobas, P. M. Campbell, G. G. Jernigan, and B. T. Jonker, Nano Lett. **13**, 668 (2013).

[13]Z. Yin *et al*., ACS Nano **6**, 74 (2012).
[14]B. Kumar *et al*., Nano Lett. **13**, 1962 (2013).
[15]K. Dolui, I. Rungger, and S. Sanvito, Phys. Rev. B **87**, 165402 (2013).
[16]B. Akdim, R. Pachter, S. S. Kim, R. R. Naik, T. R. Walsh, S. Trohalaki, G. Hong, Z. Kuang, and B. L. Farmer, ACS Appl. Mater. Interfaces **5**, 7470 (2013).
[17]Y.-Y. Chen, M. Dong, Z. Qin, X.-D. Wen, W. Fan, and J. Wang, J. Mol. Catal. A: Chem. **338**, 44 (2011).
[18]P. Hohenberg and W. Kohn, Phys. Rev. **136**, B864 (1964).
[19]W. Kohn and L. J. Sham, Phys. Rev. **140**, A1133 (1965).
[20]G. Kresse and J. Hafner, Phys. Rev. B **47**, 558 (1993).
[21]G. Kresse and J. Hafner, Surf. Sci. **459**, 287 (2000).
[22]G. Kresse and D. Joubert, Phys. Rev. B **59**, 1758 (1999).
[23]F. Mehmood, R. Pachter, W. Lu, and J. J. Boeckl, J. Phys. Chem. C **117**, 10366 (2013).
[24]J. P. Perdew, K. Burke, and M. Ernzerhof, Phys. Rev. Lett. **77**, 3865 (1996).
[25]M. Dion, H. Rydberg, E. Schröder, D. C. Langreth, and B. I. Lundqvist, Phys. Rev. Lett. **92**, 246401 (2004).
[26]H. J. Monkhorst and J. D. Pack, Phys. Rev. B **13**, 5188 (1976).
[27]R. F. W. Bader, *Atoms in Molecules: A Quantum Theory* (Oxford University Press, New York, 1990).
[28]M. Chhowalla, H. S. Shin, G. Eda, L.-J. Li, K. P. Loh, and H. Zhang, Nat. Chem. **5**, 263 (2013).
[29]S. B. Fagan, E. C. Girão, J. M. Filho, and A. G. S. Filho, Int. J. Quantum Chem. **106**, 2558 (2006).
[30]X. F. Fan, W. T. Zheng, V. Chihaia, Z. X. Shen, and J.-L. Kuo, J. Phys.: Condens. Matter **24**, 305004 (2012).
[31]T. C. Nguyen, M. Otani, and S. Okada, Phys. Rev. Lett. **106**, 106801 (2011).
[32]G. M. Rignanese, V. A. De, J. C. Charlier, X. Gonze, and R. Car, Phys. Rev. B: Condens. Matter Mater. Phys. **61**, 13250 (2000).